American Journal of Pathology, Vol. 167, No. 2, August 2005

Growth Factors, Cytokines, Cell Cycle Molecules

Lung Alveolar Septation Defects in *Ltbp-3*-Null Mice

Cristina Colarossi,* Yan Chen,* Hiroto Obata,* Vladimir Jurukovski,* Laura Fontana,* Branka Dabovic,* and Daniel B. Rifkin*†

From the Departments of Cell Biology and Medicine,† New York University School of Medicine, New York, New York*

Latent transforming growth factor (TGF)-β binding proteins (LTBPs) modulate the secretion and activation of latent TGF-β. To explore LTBP function *in vivo*, we created an *Ltbp-3*$^{-/-}$ mouse that has developmental emphysema with decreased septation in terminal alveoli. Differences in distal airspace enlargement were obvious at day 6 after birth. Secondary septation was inhibited, so by days 21 to 28 the mean linear intercept was approximately twofold greater in mutant versus control lungs. There were no differences in lung collagen and elastin, visualized by immunohistochemistry, or in myofibroblast numbers, determined by α-smooth muscle actin-positive cells, between mutant or wild-type lungs as the animals aged, other than differences associated with altered lung structure in mutant animals. However, from day 10 there was twice the number of alveolar type II cells in mutant alveoli compared to controls. At days 6 and 10, a transient enhancement in cell proliferation in the mutant lungs was observed by both 5-bromo-2′-deoxy-uridine and proliferating cell nuclear antigen labeling, accompanied by enhanced numbers of terminal dUTP nick-end labeling-positive cells at days 4, 6, and 10. Finally, there was a transient decrease in TGF-β signaling at days 4 to 6 in *Ltbp-3*$^{-/-}$ lungs. These results indicate that in the absence of Ltbp-3, a temporary decrease in TGF-β signaling in the lungs at days 4 to 6 alters cell proliferation, correlating with inhibition of septation and developmental emphysema. *(Am J Pathol 2005, 167:419–428)*

In mice, the lung buds emerge from the ventrolateral sides of the foregut endoderm during midgestation approximately at embryonic day 9.5 (somite stage 21 to 29). As the lung buds grow caudally and protrude from the gut, they invade the splanchnic mesenchyme and undergo numerous rounds of dichotomous branching to form the bronchial tree. This early developmental stage is referred to as the pseudoglandular phase and is characterized histologically by loose and thick mesenchyme surrounding tubules with relatively small lumens lined by undifferentiated columnar epithelial cells. The pseudoglandular phase lasts until embryonal day 16, when the canalicular stage commences. During this period, the terminal buds dilate and the mesenchyme thins. Further dilatation of the terminal buds and thinning of both the epithelium and the underlying mesenchyme occur in the saccular stage (E17 to postnatal day 5), when epithelial cells differentiate into type I pneumocytes and the functional gas exchange units, the sacculi, form. During alveolarization, the fourth stage, the sacculi mature into alveoli as septa form between the walls of the terminal sacs resulting in a significant increase in the gas exchange surface area. In addition, ciliated and secretory cells are now recognizable in the proximal airways, and alveolar type I and type II cells are present at distal sites. In humans alveolarization initiates prenatally, whereas in mice the process begins at postnatal day 5.[1]

Branching morphogenesis of the lung involves mesenchymal-epithelial signaling resulting in cellular proliferation, migration, and subsequent transcriptional activation of specific genes.[2] A number of molecules, including sonic hedgehog (Shh), bone morphogenetic protein-4, fibroblast growth factor (FGF)-10, transforming growth factor (TGF)-β, and retinoic acid receptor, have been implicated in the control of separation of the primitive trachea from the esophagus.[2] Deficiency of Shh results in the failure of esophageal-tracheal separation and complete failure of branching morphogenesis.[3] Activation of Gli transcription factors through Shh signal transduction pathways is important for lung morphogenesis.[4–6]

Supported by grants from the National Institutes of Health (grants CA78422 and CA34282 to D.B.R., and 32HL67542-01 and T32 CA09161 to V.J.) and a Bausch and Lomb Japanese Traveling Fellowship (to H.O.).

Accepted for publication April 29, 2005.

Present address of C.C.: Dipartimento di Medicina Sperimentale e Patologia, Viale Regina Elena 324, Rome, Italy 00161; present address of H.O.: Department of Ophthalmology, Jichi Medical School, 3311-1 Minamikawachi-machi, Kawachi-gun, Tochigi, Japan 329-0498; present address of V.J.: Department of Biochemistry and Cell Biology, SUNY at Stony Brook, Life Sciences Building, Rm. 402, Stony Brook, NY 11794-5215.

Address reprint requests to Daniel B. Rifkin, Department of Cell Biology, NYU School of Medicine, 550 First Ave., MSB 638, New York, NY 10016. E-mail: rifkid01@med.nyu.edu.

During the intermediate stages of organ development, appropriate expression of bone morphogenetic protein-4,[7,8] hepatocyte growth factor,[9] and fibroblast growth factor-10 are critical in regulating pulmonary epithelial cell proliferation, migration, and branching morphogenesis of the lung.[10] For example, fibroblast growth factor-10-null mice die immediately after birth due to disruption of pulmonary branching morphogenesis, and this phenotype is coincident with severe reduction in the expression of Shh.[10] Other studies using transgenic mice[11] have provided further evidence that the fibroblast growth factor signaling pathway is critical for airway branching and pulmonary epithelial differentiation. These and additional studies have identified distinct gene networks at proximal and distal sites along the respiratory tract and have partially defined the molecular mechanisms controlling the early development of the lung.[2]

The control of the final phase of development, alveolarization, is incompletely understood. Platelet-derived growth factor-AA, platelet-derived growth factor-BB, fibroblast growth factor, vascular endothelial growth factor, retinoic acid, glucocorticoid hormone, and TGF-β have been implicated in the regulation of this fourth phase of differentiation,[12–18] and alterations in the expression and/or concentration of any of these signaling molecules yields mice with decreased numbers of alveoli. The proper extracellular concentration and activity of the correct isoforms of TGF-β are essential to normal lung development because TGF-β affects cell differentiation, proliferation, and extracellular matrix (ECM) deposition[19–23] within the lung. Moreover, mice carrying null mutations for individual TGF-β isoforms display diverse pulmonary phenotypes. TGF-β2-null mice exhibit perinatal lethality and a range of developmental defects, including collapsed conducting airways.[24] TGF-β3 knockout mice die within 20 hours after birth and have delayed pulmonary development.[25] TGF-β1 knockout mice display severe inflammation of the lungs as well as several other organs.[26] In addition, misexpression of TGF-β1 under the control of the surfactant protein-C promoter induces neonatal lethal pulmonary hypoplasia with emphysema-like lesions and vascular hypoplasia.[27] Finally, Neptune and colleagues[16] reported that an excess of TGF-β is the cause of developmental emphysema in fibrillin-1 hypomorphic mice.

The TGF-βs are secreted as inactive complexes consisting of a disulfide-bonded homodimer of mature TGF-β associated noncovalently with the N-terminal propeptide of the TGF-β precursor.[28] The TGF-β propeptide, also called the latency-associated protein, is usually covalently attached to a latent TGF-β binding protein (LTBP) molecule. In this large latent complex, TGF-β cannot bind to its high-affinity signaling receptors and initiate signal transduction through the Smad pathway. Within the large latent complex, TGF-β is the potential signaling molecule and latency-associated protein binding confers latency to TGF-β, but the function of the LTBP is less clear.

The LTBPs 1 to 4 comprise a family of ECM proteins, three (LTBP-1, -3, and -4) of which covalently bind latent TGF-β.[29–31] The structure of the LTBPs is characterized by multiple EGF-like modules and four cysteine-rich domains called 8-cysteine (8-Cys) domains found only in LTBPs and fibrillins. LTBPs bind to the TGF-β small latent complex, which consists of TGF-β and latency-associated protein, through cysteine residues in the third 8-Cys domain.[32–34] *In vitro* experiments suggest that LTBPs may have dual roles as regulators of TGF-β bioavailability[29,35–37] and as structural components of ECM.[38] An *Ltbp-2*-null mutation in the mouse is lethal between embryonic days 3.5 to 6.5 suggesting that Ltbp-2 is important in early mouse development.[39] However, the reason for lethality in the absence of Ltbp-2 is unknown. *Ltbp-4* hypomorphic mice develop colorectal cancer and emphysema, and immunohistochemical analyses of the lungs and colons of these null mice revealed a deficit in extracellular TGF-β supporting a role for Ltbp-4 in TGF-β secretion.[37] To understand the *in vivo* biological functions of Ltbp-3, we generated *Ltbp-3*-null mice.[40] These mutant animals have a normal life span and reproduce, but they display craniofacial malformations by postnatal day 10 caused by ossification of the skull base synchondroses. Later, the animals develop osteopetrosis and osteoarthritis. These latter two phenotypes resemble those observed in murine models with impaired TGF-β signaling in bone[41–43] suggesting that in bone Ltbp-3 is required for proper TGF-β presentation.

Ltbp-3$^{-/-}$ mice were originally generated on a mixed 129SvEv/SW genetic background. In addition to these outbred animals, we also produced an inbred *Ltbp-3*$^{-/-}$ 129SvEv line. These inbred animals showed all of the reported bone defects (unpublished observations), but in addition, half of the *Ltbp-3*$^{-/-}$ mice die between 3 to 4 weeks of age,[44] there is involution of the thymus and spleen,[44] and there is an impairment of terminal alveolarization of the lungs resulting in a developmental emphysema. To elucidate the role of Ltbp-3 in lung morphogenesis, we have characterized the lung phenotype of 129SvEv *Ltbp-3*-null mice.

Materials and Methods

Mice

Ltbp-3-null mice were produced as described in Dabovic and colleagues,[36,40] and the generation of the 129/SvEv inbred line is described in Chen and colleagues.[44] Genotyping of wild-type, heterozygous, and null animals was performed as described in Dabovic and colleagues.[36] All procedures with animals were performed according to the standards approved by New York University School of Medicine Institutional Animal Care and Use Committee.

Histology and Immunohistochemistry

Mice were euthanized by cervical dislocation, the sternum and costal bones removed, and the lungs inflated through the trachea with 4% paraformaldehyde at a pressure of 25 cm H_2O for 30 minutes. After this time, the lungs were surgically removed and placed in 4% paraformaldehyde overnight. Histological analyses were con-

ducted on fixed samples that had been dehydrated through an ethanol series, cleared in xylene, and embedded in paraffin. In all experiments, tissue samples were always taken from the left lobe. Five-μm-thick sections were cut and stained with either hematoxylin and eosin (H&E) (Sigma Chemical, St. Louis, MO), modified Hart's staining solution (Sigma) for elastin, or Masson's Trichrome (Sigma) for collagen. Additional sections were immunostained with antibodies for surfactant protein B (AB378, 1:2000 dilution; Chemicon Int. Inc., Temecula, CA), for proliferating cell nuclear antigen (PCNA) (93-1143, PCNA staining kit; Zymed Laboratories, South San Francisco, CA), or for α-smooth muscle actin (α-SMA) (A2547, 1:100 dilution; Sigma). After quenching of endogenous peroxidase with 3% H_2O_2 for 20 minutes, the sections were exposed to the primary antibody. Immunodetection was performed using biotinylated anti-rabbit or anti-mouse IgG (Vector Laboratories, Burlingame, CA) as the secondary antibody. All antibodies were checked for specificity either by incubation with a blocking peptide or by incubation of sections with a nonimmune serum or isotype-matched IgG. No nonspecific reaction was observed with these treatments. For all histochemistry experiments at least two animals were included in each sample group. For PCNA quantitation, two animals in each group were sacrificed at day 6, five animals at day 10, and three animals at day 21. Two slides were prepared from each animal, the cells in 10 fields on each slide counted, and the mean and SD computed. Between 2500 to 6000 cells were counted for each animal. For surfactant B, five mice from each group were analyzed at day 10, and five mice at day 21. The percentage of positive cells was computed using five slides for each animal and 10 fields in each slide. The data are presented as the mean and SD for the percentage of positive cells in each mouse. The total number of cells counted for each mouse was 2300 to 3900.

Lung Morphometry

For morphometric studies, the mean linear intercept (MLI) was used as a measure of interalveolar wall distance. Five-μm lung sections were stained with H&E and images were captured using a $\times$10 objective with a Hammamatsu digital camera (Hamamatsu Photonics, Hamamatsu City, Japan) and Openlab 2.2.5 software. Printed images of the lung sections were prepared, and five lines were drawn across each photo: two lines connecting opposite vertices, two lines bisecting opposite sides, and one line at a random position. The length of the line drawn across the lung section was divided by the total number of alveolar intercepts encountered. Therefore, the MLI value represents the distance between intercepts. Fifty lines (10 images) were used per lung to compute the MLI.[45] For each experiment, 6 animals of each group were analyzed at day 6, 15 at day 10, and 12 at day 21. Three slides were analyzed from each animal and the number of intercepts in 10 fields for each slide computed. The numbers reported represent the mean and the SD. For secondary crest analysis, slides (n = 3) from each of five control and five null animals were analyzed (10 fields per slide at $\times$40). The numbers reported represent the mean and the SD per field.

In Situ *Hybridization*

RNA probes were prepared using the DIG RNA labeling kit (Roche, Indianapolis, IN) according to the manufacturer's instructions. To generate the probe, a fragment of DNA containing the Ltbp-3 3′ UTR was subcloned in a pBluescript SK vector. The construct was cut with restriction enzyme *Xba*I and transcribed with T7 polymerase to synthesize an anti-sense RNA probe. The control sense RNA probe was generated by T3 polymerase using the original construct cut with *Eco*RI. *In situ* hybridization was performed as described.[46] Briefly, deparaffinized sections were treated with proteinase K (20 μg/ml) for 6 minutes at room temperature, and hybridization performed overnight at 55°C in 50% formamide. The slides were washed with 2$\times$ standard saline citrate containing 50% formamide at 65°C for 30 minutes and treated with RNase A (20 μg/ml at 37°C for 30 minutes; Roche). Anti-DIG-alkaline phosphatase (AP)-coupled antibody and BM Purple AP substrate (Roche) were used to detect the signal.

5-Bromo-2′-Deoxy-Uridine (BrdU) Labeling

Six- and twenty-day-old pups were injected intraperitoneally (50 μg/g body weight) with BrdU (Sigma). Eight hours after injection, the mice were euthanized, and the lungs were removed and fixed in paraformaldehyde (4%) for immunohistochemical evaluation.[47] BrdU was revealed using the Boehringer peroxidase-conjugated anti-BrdU antibody (Boehringer-Mannheim, Indianapolis, IN) for 1 hour at room temperature. Slides were scored by counting positive cells in 40 fields at $\times$10 magnification and the values normalized to total cells in the field. Two slides were prepared for each animal and the cells in 10 fields in each slide were scored. The numbers of animals analyzed were day 6, two; day 10, five; day 21, two for both mutant and wild-type or heterozygous mice.

Terminal dUTP Nick-End Labeling (TUNEL) Apoptosis Assay

Apoptosis was detected and quantified with an In Situ Cell Death Detection kit, fluorescein (Roche Diagnostic GmbH) according to the manufacturer's directions. Briefly, paraffin-embedded formalin-fixed sections were dewaxed in xylene (5 minutes $\times$ 2), in ethanol solutions (100%, 95%, 80%, and 70%), and finally rinsed in phosphate-buffered saline (PBS) (5 minutes $\times$ 3). The sections were treated with nuclease-free proteinase K (20 μg/ml in 10 mmol/L Tris/HCl, pH 7.4) for 30 minutes at room temperature. After two washes in PBS (5 minutes $\times$ 2), 50 μl of TUNEL reaction mixture were added to each sample. As a negative control, the slides were incubated

in 50 μl of label solution without terminal transferase; as a positive control, the sections were incubated with DNase I grade I (3000 U/ml in 50 mmol/L Tris-HCl, pH 7.5, 1 mg/ml bovine serum albumin) for 10 minutes at 25°C to induce DNA strand breaks. The slides were incubated in a humidified atmosphere for 60 minutes at 37° in the dark, rinsed 3 times with PBS, and mounted in Fluoromount G (Southern Biotechnology Associates, Inc., Birmingham, AL) before direct analysis by fluorescent microscopy. Ten fields for each slide were photographed and the TUNEL-positive cells were counted in each of five slides per animal. At day 6, four animals in each group were sacrificed, and at day 10, two animals were analyzed. The total number of cells analyzed was between 5000 to 6200. The values presented represent mean and the SD.

P-Smad Labeling

Paraffin sections of lung samples were analyzed by immunohistological staining for detection of phosphorylated Smad2 and 3 (pSmad2/3) using anti-pSmad2/3 antibodies (Santa Cruz Biotechnology, Santa Cruz, CA). For detection of pSmad2/3, deparaffinized sections were treated in a Black & Decker steamer with DAKO Target Retrieval Solution (DAKO Corp., Carpinteria, CA) according to the manufacturer's protocol. After blocking with PBS/2% goat serum for 1 hour at room temperature, the samples were incubated with 1:200 dilution of the pSmad2/3 antibody and nonimmune IgG (as background control) overnight at 4°C. After washing in PBS, the samples were incubated for 1 hour at room temperature with biotinylated secondary anti-rabbit antibody. The detection of the signal and counterstaining of the nuclei was performed by incubation of the samples with streptavidin Alexa Fluor conjugate (1 μg/ml; Molecular Probes, Eugene, OR) and 4,6-diamidino-2-phenylindole (DAPI) (50 ng/ml; Roche Applied Science) in PBS for 30 minutes at room temperature. After a brief wash, the slides were mounted in Fluoromount-G and viewed using a Zeiss fluorescence microscope (Carl Zeiss, Thornwood, NY). Pictures were taken at random using a Hammamatsu digital camera and Openlab 2.2.5 software. The blue DAPI-stained nuclei were artificially colored in green using Openlab software so that the overlapping blue signals with the red stain for pSmad give a better contrast (yellow-orange). At each time point, 10 random fields from each of five slides for each genotype were counted. At day 4, six null mice and four wild-type mice were analyzed, at day 10, three mice of each genotype were analyzed, and at day 21, five mice of each genotype were analyzed. Two slides were prepared from each animal and the cells in 10 random fields in each slide scored. The results are represented as the mean and SD of the percentage pSmad2/3-positive nuclei (yellow-orange signal) of the total cell (green plus yellow-orange nuclei) number. Cells (1200 to 6000) were counted for each sample and the *P* value at day 4 between the WT and *Ltbp-3*$^{-/-}$ samples was <0.0277.

Results

Gross Abnormalities of Inbred Ltbp-3-Null Mice

At birth, inbred 129/SvEv *Ltbp-3*-null mice were indistinguishable from their wild-type and heterozygous littermates. For the first 8 to 10 days, there were no morphological or weight differences observable between wild-type and *Ltbp-3*-null mice. However, by 3 weeks of age the body weight of the mutant animals was 20 to 80% of the body weight of wild-type or heterozygous sex-matched littermates, reflecting the severity of the phenotype. Half of the homozygous null mice had a mild phenotype because they were slightly smaller (30%) than wild-type or heterozygous littermates, and these mice survived for up to 6 months. The remaining *Ltbp-3*-null animals had a severe phenotype. These animals weighed up to 20 to 75% less than wild-type or heterozygous littermates, and unlike the original outbred *Ltbp-3*-null mice, which have a normal life span, animals with the severe phenotype died at ~28 days of age. Because all of the inbred animals survived for at least 25 to 30 days, the craniofacial abnormalities originally described in the outbred mice[36,40] were clearly visible. Therefore, the penetrance of the skull defects in *Ltbp-3*$^{-/-}$ mice was 100% in both outbred and inbred mice, whereas a previously unobserved pathology resulting in premature death appeared only in the *Ltbp-3*$^{-/-}$ 129SvEV inbred mice. The fact that animals with the severe phenotype were lethargic and dyspneic at the end of the 4th week after birth suggested that the mice were dying of respiratory failure.

Distal Space Enlargement of Ltbp-3-Null Mutant Mouse Lungs

Although macroscopic analysis of the lungs from wild-type and *Ltbp-3*-null mice revealed differences in lung size starting at 2 weeks after birth, until this time, the gross morphology, number of lobes, lung shape, and lung/body weight ratios were similar between mutant and wild-type or heterozygous littermates (data not shown). Histological analysis of the lungs of *Ltbp-3*-null mice was performed on mice 4, 6, 8, 10, 15, 18, and 20 to 30 days of age. Throughout this period, the proximal airways and vessels appeared normal. No differences between mutant and normal lungs were noted until days 5 to 6 of postnatal life. At day 6, the normal lungs are highly branched, and the walls of the saccules have multiple short buds that elongate to form the secondary septa. In homozygous mutant mouse saccules at day 6, the buds were either short or absent compared to the saccules of wild-type mice (Figure 1, day 6). No differences between heterozygous and wild-type animals were observed by histological analysis or by the analyses for specific markers described below. This is consistent with what has been described earlier for other *Ltbp-3*$^{-/-}$ phenotypes, which are obvious only in the homozygote.[32,36,40] The decrease of secondary septa continued as the mice aged and resulted in a progressive increase in the size of

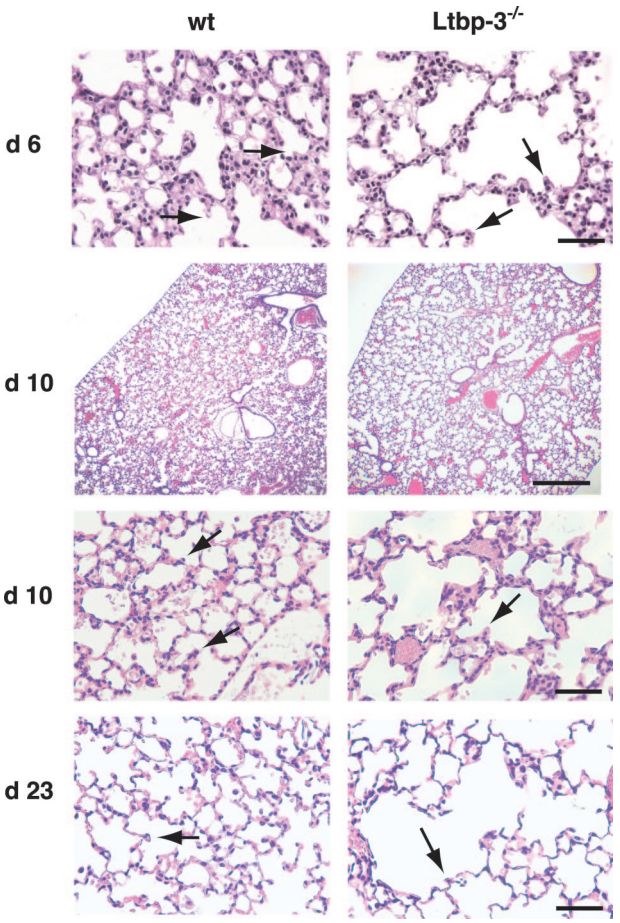

Figure 1. Histology of lungs from wild-type and *Ltbp-3*$^{-/-}$ mice at days 6, 10, and 23 after birth. The **arrows** point to the initial budding septae. Scale bars: 500 μm (**row 2**); 100 μm (**rows 1, 3, and 4**).

the alveolar ducts and their alveolar sacs as the lungs developed (Figure 1, day 10). At this time, clear differences between the control and null lungs are evident at low as well as at high magnification (Figure 1). By day 23, the histological pattern in mutant lungs was characterized by a reduced number of airspaces and by a continued progressive increase in size of the alveolar ducts (Figure 1).

To quantitate differences in alveolarization, the MLIs in mutant and wild-type or heterozygous lungs were compared. This measurement quantitates the distance between alveolar septae across the lung. Therefore, fewer septa will yield larger MLI intercept numbers. The mutant animals had a distal airspace enlargement compared to wild-type animals (Figure 1). At day 6 after birth the MLI in mutant lungs was 1.53-fold larger than that of wild-type lungs (MLI: 2.44 $\pm$ 0.05 versus 1.59 $\pm$ 0.19; $P > 0.007$). The size of the airway space was 1.7 times bigger (MLI: 2.50 $\pm$ 0.48 versus 1.49 $\pm$ 0.27; $P > 0.0003$) in mutant versus wild-type lungs at day 10, and increased up to 2.03-fold (MLI: 2.42 $\pm$ 0.13 versus 1.2 $\pm$ 0.21; $P > 4.1$ E-06) by day 23. Thus, the 129/SvE *Ltbp-3*$^{-/-}$ mice with the severe phenotype had a progressive developmental emphysema resulting from an inhibition of septation during the alveolarization phase of lung development.

As a second approach to computing differences in alveolization of control and mutant lungs, we counted the numbers of secondary crests in specimens from the two mouse types. At day 6 after birth control mice had 24.9 $\pm$ 2.6 crests per field, whereas the null mice had 14.9 $\pm$ 0.46 ($P > 1.2$ E-06). By day 21, the control mice had 41.2 $\pm$ 3.6 and the null mice had 26.4 $\pm$ 1.5 crests per field ($P > 0.06$) indicating diminished alveolar septation in the *Ltbp-3*$^{-/-}$ mice.

Analysis of Alveologenic Factors

We previously reported that *Ltbp-3* is expressed in the lung at E13 and E16 based on *in situ* hybridization assays.[40] Northern blot analyses using RNAs obtained from wild-type mice confirmed the presence of Ltbp-3 mRNA in adult lung tissue.[36] To identify the cell type(s) that expresses Ltbp-3, we performed *in situ* hybridization analyses on lung sections from pups and adult mice using an *Ltbp-3*-specific probe. At day 10, the *Ltbp-3* mRNA was diffusely expressed in the pulmonary parenchyma and in the alveolae, mainly in alveolar type II cells (Figure 2A).

During normal alveologenesis, differentiation from epithelial to alveolar cells precedes terminal septation.[2] Thus, the early defects in alveologenesis may result from deficient alveolar cell production. To determine whether epithelial cell differentiation is affected in the *Ltbp-3*-null inbred mice, immunohistochemical staining using an antibody to surfactant protein B, a marker of differentiated alveolar type II and Clara cells, was performed. The staining patterns of lungs from mutant and heterozygous animals revealed no differences in either the localization or concentration of antigen in distal airways at days 4 or 21 (data not shown). However, specimens from 10-day-old mice displayed increases in type II cells in the mutant lungs compared to wild-type or heterozygous lungs (Figure 2B). Quantitation of the percentage of cells positive for surfactant B at day 10 indicated that the mutant lungs contained almost twice the percentage of positive cells as wild-type lungs (20.6 $\pm$ 0.96% versus 12.1 $\pm$ 0.34%; $P < 0.0013$). Electron microscopic analysis of normal and mutant lungs showed that the alveolar type II cells contained lamellar bodies indicating that surfactant was produced (data not shown). These results suggest that the differentiation of the distal epithelium is transiently affected between days 4 and 21 by the lack of Ltbp-3.

Elastin is important for the proper development and function of the lung.[48,49] Elastin, a structural protein of the ECM, confers elastic properties on the pulmonary alveolar interstitium. Mice deficient in Ltbp-4 show a fragmentation of their elastic fibers associated with a developmental emphysema.[37] Moreover, as TGF-β affects elastin gene expression[22,50], alterations in TGF-β binding proteins might be expected to affect elastin levels. To evaluate whether the pulmonary abnormalities in *Ltbp-3*-null mice reflect alterations in elastin fiber structure and deposition, we examined the distribution and morphology of the elastic fibers in lung sections prepared with Hart's stain. The number of elastin fibers and the intensity of the

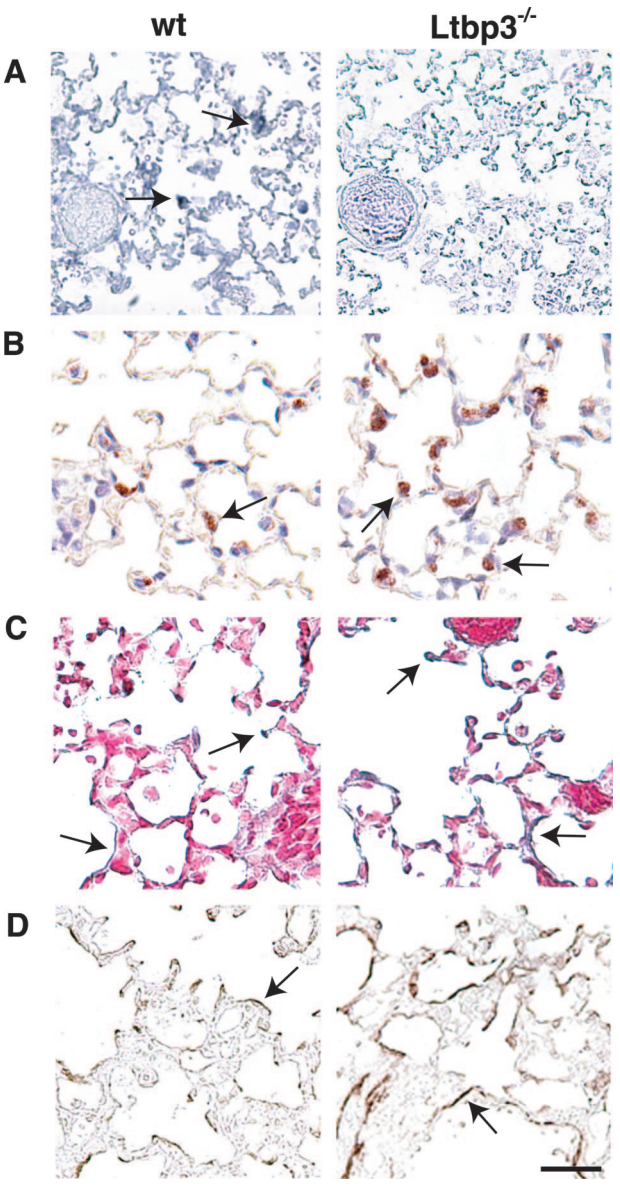

Figure 2. Lung cell markers. **A:** *Ltbp-3* expression in the lung. *In situ* hybridization using a probe from the 3′ UTR of Ltbp-3. *Ltbp-3* transcripts were detected in alveolar type II cells (**arrows**). There was no signal in *Ltbp-3*$^{-/-}$ lungs. **B:** Surfactant B levels in wild-type and mutant lungs. Lung samples were analyzed at 10 days by immunohistochemistry for surfactant-containing cells as described in Materials and Methods. *Ltbp-3*$^{-/-}$ lungs show more surfactant B-producing cells than wild-type lungs at this day. **Arrows** point to positive cells. A representative experiment is shown. **C:** Elastin staining in the lungs of 10-day-old wild-type and *Ltbp-3*$^{-/-}$ lungs. The **arrows** point to the elastin at the tips of the newly forming septa. The elastin does not appear to be fragmented. **D:** Staining for α-SMA (**arrows**) in wild-type and mutant lungs at day 10. Similar patterns were observed at days 6 and 21 (data not shown). Each assay was repeated at least five times. Representative experiments are shown.

staining was similar in mutant and wild-type mice (Figure 2C). Elastin was detected in the mesenchyme surrounding the airways and blood vessels as well as at the tips of the growing septa, even though the number of septa were diminished in mutant lungs. Analysis of mutant and wild-type lungs by electron microscopy confirmed the presence of elastin and the absence of fragmentation of the elastic fibers (data not shown).

Because myofibroblasts have been implicated in the control of lung development,[13] we examined the number and distribution of these cells by staining specimens with an antibody against α-SMA. Immunohistochemical analysis for α-SMA revealed that the number of myofibroblasts (not shown) and distribution of α-SMA (Figure 2D) is equivalent in lungs from inbred *Ltbp-3*-null mice compared to wild-type animals, apart from those structural changes that reflect the differences in alveolarization. Because collagen gene expression is highly sensitive to TGF-β levels, we examined the collagen content and distribution in lungs from mutant and normal animals by Masson's Trichrome staining. No significant differences were found in collagen distribution or staining intensity other than those relating to the primary structural differences in the lungs (data not shown).

Proliferation and Apoptosis

There is rapid cell proliferation during early and mid-gestational lung organogenesis. At postnatal days 2 to 4, the number of proliferating cells substantially increases to support postnatal growth.[51] To examine proliferation in normal and mutant lungs, we labeled the cells by intraperitoneal injection of BrdU. At day 21, the number of BrdU-positive cells, revealed by immunohistochemistry was equivalent in homozygous null mice compared to wild-type or heterozygous mice (Table 1). However, a significant increase in BrdU-positive cells was apparent in the mutant lungs at days 6 and 10, despite the smaller total number of cells resulting from the reduced alveolarization. Similar data were obtained using immunostaining for PCNA, another marker of dividing cells (Table 1). Therefore, there appears to be transient enhanced proliferation of alveolar type II cells in mutant mice at the approximate mid-point in normal lung alveolarization.

The observed increases in cell proliferation as evidenced by PCNA and BrdU labeling appeared to be in contradiction with the obvious decrease in cellularity of the *Ltbp-3*-null lungs. We reasoned that enhanced apoptosis in the mutant lungs might account for the overall decreased number of lung cells. Therefore, we measured the amount of apoptosis in wild-type and mutant lungs using the TUNEL assay (Table 1). Increased numbers of TUNEL-positive cells were detected both at days 4 to 6 and at day 10 in mutant lungs compared to wild-type or heterozygous lungs. At day 10 there was significant variability in the mutant samples. The reason for this is unclear but may reflect differences between mild and severe phenotypes that cannot be distinguished at this age.

PSmad2/3

The loss of either Ltbp-3 or Ltbp-4 is associated with decreases in TGF-β activity in bone,[36] lung,[37] and colon.[37] Therefore, we attempted to determine whether decreased levels of TGF-β could be observed in mutant 129/SvEv versus wild-type lungs. We were unable to detect alterations in TGF-β levels by direct immunohistochemistry for TGF-β (data not shown). Therefore, we

Table 1. Cell Growth in Wild-Type and *Ltbp-3*$^{-/-}$ Lungs

Day	BrdU		PCNA		TUNEL	
	WT	*Ltbp-3*$^{-/-}$	WT	*Ltbp-3*$^{-/-}$	WT	*Ltbp-3*$^{-/-}$
6	3.03 ± 0.028	6.46 ± 0.232	5.17 ± 0.033	10.01 ± 0.124	1.318 ± 0.13	2.656 ± 0.110
10	3.33 ± 0.90	6.35 ± 0.11	5.37 ± 0.242	11.15 ± 0.224	0.737 ± 0.079	1.63 ± 0.042
21	1.32 ± 0.012	1.378 ± 0.109	1.75 ± 0.022	2.18 ± 0.142	N.D.	N.D.

Data are presented as the percentage of total cells that stained positive for the specific marker tested. Data represent result averages and SE. For each experiment, five slides were used and 10 fields per slide were counted. The number of animals used for each experimental group is given in Materials and Methods. N.D., not done. The *P* values were BrdU: day 6, <0.033; day 10, <2E-06; day 21, <0.359; PCNA: day 6, <0.005; day 10, <7.8 E-6; day 21, <0.257; TUNEL: day 6, <0.0008; day 10, <0.067.

used an indirect approach and measured the distribution of Smad2/3. Smad2 and Smad3 are normally found in the cytoplasm. On TGF-β signaling, the two Smads are phosphorylated (pSmad2/3), and they move into the nucleus.[52] Therefore, we examined the distribution of pSmad2/3 in the lungs of wild-type and mutant mice (Figure 3). At days 4 to 6 after birth, the samples from the mutant lungs had significantly less nuclear pSmad2/3 than cells from wild-type lungs (27.7 ± 6.21% versus 37.9 ± 7.23%; $P < 0.028$). Decreased levels of nuclear pSmad2/3 in mutant lungs were not observed at the later time points (data not shown). Therefore, latent TGF-β activation and TGF-β signaling appear to be altered only at early times during lung development in *Ltbp-3*-null animals. These early differences may result in the subsequent morphological effects.

Discussion

In this article, we describe an analysis of the development of the alveoli in *Ltbp-3*-null mice. The *Ltbp-3*-null mutation, when placed in a 129SvEv background, produces animals with developmental emphysema. Fifty percent of *Ltbp-3*$^{-/-}$ animals display severe emphysema and die at ~day 30 after birth; the other half has a milder phenotype as these animals live longer, are not as severely growth impaired, and have a moderate emphysema. The emphysematous phenotype is observed in all

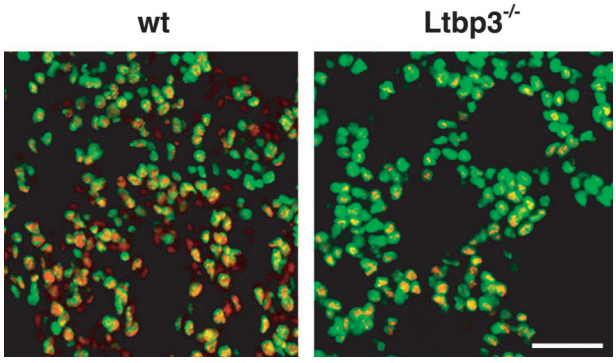

Figure 3. pSmad2/3 nuclear staining in wild-type and *Ltbp-3*$^{-/-}$ lungs. To visualize TGF-β signaling in the lungs of wild-type and mutant mice, lung sections were stained with an antibody to pSmad2/3 and Alexa Fluor and the numbers of nuclei with positive staining computed. The positive pSmad2/3 signal is red. Cell nuclei are stained with DAPI and the normal blue product was artificially colored green. Therefore, cells with nuclear pSmad2/3 appear yellow-orange because of the red-green overlap. The data from 4-day-old animals are presented. The assay was performed four times with similar results.

inbred mutant animals, to varying degrees, and is also apparent in those outbred animals with a severe skeletal phenotype (data not shown). Why the lung phenotype is more severe in the 129SvEv background is unclear, but the effect of modifier genes on TGF-β-related phenotypes has been described.[53]

Our analysis of developing lungs in inbred *Ltbp-3*-null mice suggests the following sequence of events during lung maturation. At days 4 to 6 in mutant animal lungs there is a decrease in the level of nuclear pSmad2/3 indicating diminished TGF-β signaling. This alteration in pSmad levels is transient because no differences between mutant and wild-type lungs were observed at days 10 or 21. The change in TGF-β signaling corresponds to the earliest time when morphological differences in the lungs of the two animal types can be discerned. At days 4 to 6, there is also an increase in the number of TUNEL-positive cells in Ltbp-3-null compared to wild-type lungs. Because TGF-β is known to suppress apoptosis,[54] the enhanced number of TUNEL-positive cells may also reflect decreased TGF-β signaling. (It should be appreciated that the TUNEL assay would also detect DNA fragmentation caused by other nonapoptotic processes such as necrosis. However, because there was no indication of necrosis, we consider this possibility unlikely.) At day 10, pSmad2/3 levels have normalized in the mutant lungs, but the enhanced rate of apoptosis continues. At this time, differences in mitotic rate between mutant and wild-type lungs become apparent as measured by both BrdU incorporation and PCNA staining. The number of cells producing surfactant B is also increased in the *Ltbp-3*-null compared to wild-type lungs on day 10. We suggest that the increase in mitosis is an attempt of the lung to compensate for cell loss at the earlier days (days 4 to 6). Enhanced cell proliferation is observed during the progression of adult destructive emphysema[55] and may be a general property of the lung in response to an imbalance of different cell types. The increase in surfactant-containing alveolar type II cells is the product of the higher mitotic rate. The number of alveolar type II cells remains high even though the absolute number of cells in the distal part of the lung is considerably lower in mutant versus wild-type lungs. It is interesting that the number of myofibroblasts, which have been implicated in the differentiation of the lung[56] and which can be affected by TGF-β levels,[54] is equivalent in normal and mutant lungs at the times analyzed.

The TGF-βs contribute to lung differentiation at multiple points because disturbances in their action result in vari-

able phenotypes depending on the period in which the signaling change occurs and whether there is underexpression or overexpression of a specific TGF-β isoform.[16,24,25,37] In the animals described here, TGF-β action has not been directly permuted. Instead, we have created mice deficient in Ltbp-3. Ltbp is thought to assist in the release of TGF-β from cells, to sequester latent TGF-β in the ECM, and to participate in the activation of latent TGF-β by certain activators.[28,57] *In situ* hybridization assays indicate high levels of *Ltbp-3* expression by alveolar type II and Clara cells of the developing and newborn lung. Our studies reveal that *Ltbp-3*-null mice have decreased TGF-β signaling between days 4 to 6 after birth, but this difference is transient. Our inability to detect persistent differences in TGF-β signaling at later times during alveolarization indicates that other molecules or mechanisms for controlling TGF-β activation are operative at these times.

With respect to how latent TGF-β is activated in the lung, it is important to consider the two mouse models most similar to *Ltbp-3*$^{-/-}$ mice in both their physiological outcome and their genetic manipulation: fibrillin-1 and *Ltbp-4* hypomorphic mice. Fibrillin-1 hypomorphic mice develop an emphysema comparable to that of *Ltbp-3*-null mice with respect to age and histology.[16] However, there are several important differences between the emphysema in fibrillin-1 hypomorphic and *Ltbp-3*-null mice. The lack of alveolarization is more pronounced in the fibrillin-1 hypomorphic mice than in *Ltbp-3*-null mice because the emphysema is evident at birth and the mice eventually develop an inflammatory response, Moreover, the lack of septation in fibrillin-1 hypomorphic mice is associated with increased, not decreased, TGF-β signaling. The increase in TGF-β signaling is persistent and has been measured at multiple days, although the affected mice die by days 10 to 14.[16] The authors propose that in fibrillin-1 hypomorphic animals LTBP in the large latent complex is unable to associate with fibrillin-1-containing microfibrils. The lack of proper sequestration permits inappropriate activation of latent TGF-β because of its mislocalization, and these high levels of TGF-β impair cell proliferation.

Ltbp-4 hypomorphic mice also develop an emphysema that is similar but not identical to that of *Ltbp-3*-null animals. This emphysema occurs earlier than that in *Ltbp-3*$^{-/-}$ mice because the disease initiates at the saccular phase. *Ltbp-4* hypomorphic animals do not die early, although they do develop additional pathologies.[37] The cells in the lung release less TGF-β, implying that the emphysema is related to a TGF-β deficit. Thus, although fibrillin-1 and *Ltbp-4* hypomorphic lungs are similar histologically, the causes of impaired alveolarization are quite different; enhanced active TGF-β in fibrillin-1 hypomorphic mice versus decreased TGF-β in *Ltbp-4* hypomorphic mice. Finally, unlike the lungs of fibrillin-1 hypomorphic and *Ltbp-3*-null mice, the elastin in the lungs of *Ltbp-4* hypomorphic animals is fragmented. Because elastin is reported to be crucial for septa formation,[56] the decrease in organized elastic fibrils may explain the *Ltbp-4* mutant lung phenotype.

How can these three different mutations, *Ltbp-3*$^{-/-}$, *Ltbp-4* hypomorph, and fibrillin-1 hypomorph, cause phenotypes that are similar but not identical? We believe that the explanation derives from the pleiotropic action of TGF-β, its bimodal activity in certain circumstances, and the unique manner in which TGF-β is presented in the extracellular milieu. Within the developing lung, the TGF-β isoforms have multiple activities. The TGF-βs are potent modulators of matrix synthesis both by enhancing the expression of multiple ECM molecules including elastin, and by regulating ECM catabolism.[58] In addition, TGF-β has both growth inhibitory and growth promoting activities depending on the concentration of the growth factor, the cell target, the matrix, and the overall constellation of growth factors. Thus, decreased levels of TGF-β, as reported for *Ltbp-3* and *Ltbp-4* mutant mice, may prevent lung cell differentiation, whereas excess TGF-β, as reported for fibrillin-1 hypomorphic animals, may inhibit normal lung cell proliferation.

TGF-β can associate with both Ltbp-3 and Ltbp-4 in the newborn lung. Ltbp-1 is also expressed in the lung[59] yielding a situation in which three molecules that bind TGF-β are all produced in the same tissue. Although expression of these TGF-β mediators may be restricted to unique cell types, numerous cells *in vitro* have been shown to produce multiple LTBPs.[29] We hypothesize that TGF-β complexes containing different LTBPs and produced by the same cell are not redundant and are localized to unique sites within the ECM. The differential localization of the large latent complex based on LTBP isoform permits unique activation mechanisms to generate active TGF-β in both a temporal and spatial-specific manner. This hypothesis also suggests that the inappropriate presentation of soluble latent TGF-β, as in the fibrillin-1 hypomorphic mouse, might yield inappropriate, excessive activation and TGF-β signaling. Although this hypothesis has several attractive features, it remains to be proven experimentally.

Acknowledgment

We thank Byron Arias for assistance with sectioning.

References

1. Tenhave-Opbroek A: The development of the lung in mammals: an analysis of concepts and findings. Am J Anat 1981, 152:201–219
2. Warburton D, Schwarz M, Tefft D, Flores-Delgado G, Anderson KD, Cardoso WV: The molecular basis of lung morphogenesis. Mech Dev 2000, 92:55–81
3. Litingtung Y, Lei L, Westphal H, Chiang C: Sonic hedgehog is essential to foregut development. Nat Genet 1998, 20:58–61
4. Grindley JC, Bellusci S, Perkins D, Hogan BL: Evidence for the involvement of the Gli gene family in embryonic mouse lung development. Dev Biol 1997, 188:337–348
5. Motoyama J, Liu J, Mo R, Ding Q, Post M, Hui CC: Essential function of Gli2 and Gli3 in the formation of lung, trachea and oesophagus. Nat Genet 1998, 20:54–57
6. Sasaki H, Nishizaki Y, Hui C, Nakafuku M, Kondoh H: Regulation of Gli2 and Gli3 activities by an amino-terminal repression domain: implication of Gli2 and Gli3 as primary mediators of Shh signaling. Development 1999, 126:3915–3924

7. Weaver M, Yingling JM, Dunn NR, Bellusci S, Hogan BL: Bmp signaling regulates proximal-distal differentiation of endoderm in mouse lung development. Development 1999, 126:4005–4015
8. Bellusci S, Henderson R, Winnier G, Oikawa T, Hogan BL: Evidence from normal expression and targeted misexpression that bone morphogenetic protein (Bmp-4) plays a role in mouse embryonic lung morphogenesis. Development 1996, 122:1693–1702
9. Ohmichi H, Koshimizu U, Matsumoto K, Nakamura T: Hepatocyte growth factor (HGF) acts as a mesenchyme-derived morphogenic factor during fetal lung development. Development 1998, 125: 1315–1324
10. Sekine K, Ohuchi H, Fujiwara M, Yamasaki M, Yoshizawa T, Sato T, Yagishita N, Matsui D, Koga Y, Itoh N, Kato S: Fgf10 is essential for limb and lung formation. Nat Genet 1999, 21:138–141
11. Peters K, Werner S, Liao X, Wert S, Whitsett J, Williams L: Targeted expression of a dominant negative FGF receptor blocks branching morphogenesis and epithelial differentiation of the mouse lung. EMBO J 1994, 13:3296–3301
12. Tschanz SA, Damke BM, Burri PH: Influence of postnatally administered glucocorticoids on rat lung growth. Biol Neonate 1995, 68:229–245
13. Bostrom H, Willetts K, Pekny M, Leveen P, Lindahl P, Hedstrand H, Pekna M, Hellstrom M, Gebre-Medhin S, Schalling M, Nilsson M, Kurland S, Tornell J, Heath JK, Betsholtz C: PDGF-A signaling is a critical event in lung alveolar myofibroblast development and alveogenesis. Cell 1996, 85:863–873
14. Massaro GD, Massaro D: Postnatal treatment with retinoic acid increases the number of pulmonary alveoli in rats. Am J Physiol 1996, 270:L305–L310
15. Weinstein M, Xu X, Ohyama K, Deng CX: FGFR-3 and FGFR-4 function cooperatively to direct alveogenesis in the murine lung. Development 1998, 125:3615–3623
16. Neptune ER, Frischmeyer PA, Arking DE, Myers L, Bunton TE, Gayraud B, Ramirez F, Sakai LY, Dietz HC: Dysregulation of TGF-beta activation contributes to pathogenesis in Marfan syndrome. Nat Genet 2003, 33:407–411
17. Buch S, Han RN, Cabacungan J, Wang J, Yuan S, Belcastro R, Deimling J, Jankov R, Luo X, Lye SJ, Post M, Tanswell AK: Changes in expression of platelet-derived growth factor and its receptors in the lungs of newborn rats exposed to air or 60% O(2). Pediatr Res 2000, 48:423–433
18. Jakkula M, Le Cras TD, Gebb S, Hirth KP, Tuder RM, Voelkel NF, Abman SH: Inhibition of angiogenesis decreases alveolarization in the developing rat lung. Am J Physiol 2000, 279:L600–L607
19. Maniscalco WM, Sinkin RA, Watkins RH, Campbell MH: Transforming growth factor-beta 1 modulates type II cell fibronectin and surfactant protein C expression. Am J Physiol 1994, 267:L569–L577
20. Zhou L, Dey CR, Wert SE, Whitsett JA: Arrested lung morphogenesis in transgenic mice bearing an SP-C-TGF-beta1 chimeric. Dev Biol 1996, 175:227–238
21. Shanker G, Olson D, Bone R, Sawhney R: Regulation of extracellular matrix proteins by transforming growth factor beta1 in cultured pulmonary endothelial cells. Cell Biol Int 1999, 23:61–72
22. Kucich U, Rosenbloom JC, Abrams WR, Bashir MM, Rosenbloom J: Stabilization of elastin mRNA by TGF-beta: initial characterization of signaling pathway. Am J Respir Cell Mol Biol 1997, 17:10–16
23. McGowan SE, McNamer R: Transforming growth factor-beta increases elastin production by neonatal rat lung fibroblasts. Am J Respir Cell Mol Biol 1990, 3:369–376
24. Sanford LP, Ormsby I, Gittenberger-de Groot AC, Sariola H, Friedman R, Boivin GP, Cardell EL, Doetschman T: TGF-beta2 knockout mice have multiple developmental defects that are non-overlapping with other TGFbeta knockout phenotypes. Development 1997, 124:2659–2670
25. Kaartinen V, Voncken JW, Shuler C, Warburton D, Bu D, Heisterkamp N, Groffen J: Abnormal lung development and cleft palate in mice lacking TGF-beta 3 indicates defects of epithelial-mesenchymal interaction. Nat Genet 1995, 11:415–421
26. Kulkarni AB, Huh CG, Becker D, Geiser A, Lyght M, Flanders KC, Roberts AB, Sporn MB, Ward JM, Karlsson S: Transforming growth factor beta 1 null mutation in mice causes excessive inflammatory response and early death. Proc Natl Acad Sci USA 1993, 90:770–774
27. Zeng X, Gray M, Stahlman MT, Whitsett JA: TGF-beta1 perturbs vascular development and inhibits epithelial differentiation in fetal lung in vivo. Dev Dyn 2001, 221:289–301
28. Annes JP, Munger JS, Rifkin DB: Making sense of latent TGFbeta activation. J Cell Sci 2003, 116:217–224
29. Koli K, Saharinen J, Hyytiainen M, Penttinen C, Keski-Oja J: Latency, activation, and binding proteins of TGF-beta. Microsc Res Tech 2001, 52:354–362
30. Rifkin DB: Latent TGF-beta binding proteins: orchestrators of TGF-beta availability. J Biol Chem 2005, 280:7409–7412
31. Hyytiainen M, Penttinen C, Keski-Oja J: Latent TGF-beta binding proteins: extracellular matrix association and roles in TGF-beta activation. Crit Rev Clin Lab Sci 2004, 41:233–264
32. Gleizes PE, Beavis RC, Mazzieri R, Shen B, Rifkin DB: Identification and characterization of an eight-cysteine repeat of the latent transforming growth factor-beta binding protein-1 that mediates bonding to the latent transforming growth factor-beta1. J Biol Chem 1996, 271:29891–29896
33. Saharinen J, Taipale J, Keski-Oja J: Association of the small latent transforming growth factor-beta with an eight cysteine repeat of its binding protein LTBP-1. EMBO J 1996, 15:245–253
34. Saharinen J, Keski-Oja J: Specific sequence motif of 8-Cys repeats of TGF-beta binding proteins, LTBPs, creates a hydrophobic interaction surface for binding of small latent TGF-beta. Mol Biol Cell 2000, 11:2691–2704
35. Miyazono K, Olofsson A, Colosetti P, Heldin CH: A role of the latent TGF-beta 1-binding protein in the assembly and secretion of TGF-beta 1. EMBO J 1991, 10:1091–1101
36. Dabovic B, Chen Y, Colarossi C, Obata H, Zambuto L, Perle MA, Rifkin DB: Bone abnormalities in latent TGF-[beta] binding protein (Ltbp)-3-null mice indicate a role for Ltbp-3 in modulating TGF-[beta] bioavailability. J Cell Biol 2002, 156:227–232
37. Sterner-Kock A, Thorey IS, Koli K, Wempe F, Otte J, Bangsow T, Kuhlmeier K, Kirchner T, Jin S, Keski-Oja J, Von Melchner H: Disruption of the gene encoding the latent transforming growth factor-beta binding protein 4 (LTBP-4) causes abnormal lung development, cardiomyopathy, and colorectal cancer. Genes Dev 2002, 16:2264–2273
38. Dallas SL, Miyazono K, Skerry TM, Mundy GR, Bonewald LF: Dual role for the latent transforming growth factor-beta binding protein in storage of latent TGF-beta in the extracellular matrix and as a structural matrix protein. J Cell Biol 1995, 131:539–549
39. Shipley JM, Mecham RP, Maus E, Bonadio J, Rosenbloom J, McCarthy RT, Baumann ML, Frankfater C, Segade F, Shapiro SD: Developmental expression of latent transforming growth factor beta binding protein 2 and its requirement early in mouse development. Mol Cell Biol 2000, 20:4879–4887
40. Dabovic B, Chen Y, Colarossi C, Zambuto L, Obata H, Rifkin DB: Bone defects in latent TGF-beta binding protein (Ltbp)-3 null mice; a role for Ltbp in TGF-beta presentation. J Endocrinol 2002, 175:129–141
41. Serra R, Johnson M, Filvaroff EH, LaBorde J, Sheehan DM, Derynck R, Moses HL: Expression of a truncated, kinase-defective TGF-beta type II receptor in mouse skeletal tissue promotes terminal chondrocyte differentiation and osteoarthritis. J Cell Biol 1997, 139:541–552
42. Filvaroff E, Erlebacher A, Ye J, Gitelman SE, Lotz J, Heillman M, Derynck R: Inhibition of TGF-beta receptor signaling in osteoblasts leads to decreased bone remodeling and increased trabecular bone mass. Development 1999, 126:4267–4279
43. Yang X, Chen L, Xu X, Li C, Huang C, Deng CX: TGF-beta/Smad3 signals repress chondrocyte hypertrophic differentiation and are required for maintaining articular cartilage. J Cell Biol 2001, 153:35–46
44. Chen Y, Dabovic B, Colarossi C, Santori FR, Lilic M, Vukmanovic S, Rifkin DB: Growth retardation as well as spleen and thymus involution in latent TGF-beta binding protein (Ltbp)-3 null mice. J Cell Physiol 2003, 196:319–325
45. Thurlbeck WM: Measurement of pulmonary emphysema. Am Rev Respir Dis 1967, 95:752–764
46. Wassarman KM, Lewandoski M, Campbell K, Joyner AL, Rubenstein JL, Martinez S, Martin GR: Specification of the anterior hindbrain and establishment of a normal mid/hindbrain organizer is dependent on Gbx2 gene function. Development 1997, 124:2923–2934
47. Tsujimura A, Koikawa Y, Salm S, Takao T, Coetzee S, Moscatelli D, Shapiro E, Lepor H, Sun TT, Wilson EL: Proximal location of mouse

prostate epithelial stem cells: a model of prostatic homeostasis. J Cell Biol 2002, 157:1257–1265
48. Noguchi A, Reddy R, Kursar JD, Parks WC, Mecham RP: Smooth muscle isoactin and elastin in fetal bovine lung. Exp Lung Res 1989, 15:537–552
49. Wendel DP, Taylor DG, Albertine KH, Keating MT, Li DY: Impaired distal airway development in mice lacking elastin. Am J Respir Cell Mol Biol 2000, 23:320–326
50. Parks WC: Posttranscriptional regulation of lung elastin production. Am J Respir Cell Mol Biol 1997, 17:1–2
51. Kauffman SL: Kinetics of pulmonary epithelial proliferation during prenatal growth of the mouse lung. Anat Rec 1975, 183:393–403
52. Shi Y, Massague J: Mechanisms of TGF-beta signaling from cell membrane to the nucleus. Cell 2003, 113:685–700
53. Bourdeau A, Faughnan ME, McDonald ML, Paterson AD, Wanless IR, Letarte M: Potential role of modifier genes influencing transforming growth factor-beta1 levels in the development of vascular defects in endoglin heterozygous mice with hereditary hemorrhagic telangiectasia. Am J Pathol 2001, 158:2011–2020
54. Zhang HY, Phan SH: Inhibition of myofibroblast apoptosis by transforming growth factor beta(1). Am J Respir Cell Mol Biol 1999, 21:658–665
55. Yokohori N, Aoshiba K, Nagai A: Increased levels of cell death and proliferation in alveolar wall cells in patients with pulmonary emphysema. Chest 2004, 125:626–632
56. Vaccaro C, Brody JS: Ultrastructure of developing alveoli. I. The role of the interstitial fibroblast. Anat Rec 1978, 192:467–479
57. Annes JP, Chen Y, Munger JS, Rifkin DB: Integrin alphaVbeta6-mediated activation of latent TGF-beta requires the latent TGF-beta binding protein-1. J Cell Biol 2004, 165:723–734
58. Taipale J, Saharinen J, Keski-Oja J: Extracellular matrix-associated transforming growth factor-beta: role in cancer cell growth and invasion. Adv Cancer Res 1998, 75:87–134
59. Noguera I, Obata H, Gualandris A, Cowin P, Rifkin DB: Molecular cloning of the mouse Ltbp-1 gene reveals tissue specific expression of alternatively spliced forms. Gene 2003, 308:31–41